**Dynamik**

**Statik**

Technische
Universität
Berlin

TU berlin

# Decision making in structural engineering problems under polymorphic uncertainty

# -

# A benchmark proposal

Y. Petryna[*1], M. Drieschner[1], P. Kähler[1]

Version 3: June 17, 2020

[*]Correspondence: Y. Petryna: yuriy.petryna@tu-berlin.de

[1]Technische Universität Berlin, Faculty VI Planning Building Environment, Department of Civil Engineering, Chair of Structural Mechanics, Gustav-Meyer-Allee 25, 13355 Berlin, Germany

# Decision making in structural engineering problems under polymorphic uncertainty

# -

# A benchmark proposal

## Y. Petryna, M. Drieschner, P. Kähler

**Abstract**

The treatment of diverse uncertainties is an important challenge in structural engineering problems, especially from the viewpoint of realistic analysis. Inaccuracy and variability are always present and have to be quantified by either probabilistic, possibilistic, polymorphic or other uncertainty approaches. Regardless to the applied uncertainty quantification method, the numerical predictions have to be useful for structural assessment and decision making. The authors propose in this contribution a benchmark example of a portal frame structure including various uncertainties. The goal of this benchmark study is to compare justifications and decisions provided by different uncertainty models with respect to clear challenges of decision making with and without measurements, data assimilation and design. The engineering problem itself is simple enough to understand and complex enough not to be reduced to a simple formula with uncertain parameters.

**Keywords**     *benchmark; polymorphic uncertainties; portal frame; decision making; data assimilation; design under uncertainties*

## 1   Introduction and goals

Engineering structures are often objects of high complexity and have to reliably operate in diverse environment and under extreme loading conditions. Therefore, they are subject of thorough design, detailing and optimization. Additional challenges arise during service life, mainly due to damage, aging and deterioration, which require decisions upon safety, operation, repair and maintenance. At that, numerous aspects are subject of polymorphic uncertainties which can be generally subdivided into epistemic and aleatory ones. Engineering experience to deal with aleatory uncertainties by probabilistic methods is already reflected in design codes of practice. In contrast, creating uncertainty models for epistemic uncertainties is far from standard and needs systematic studies and benchmarks. The goal of this benchmark study is to compare justifications and decisions provided by different uncertainty models with respect to challenges of decision making with and without measurements, data assimilation and design.

Dealing with uncertainties has been subject of research in several fields like weather and climate predictions [22], geosciences [9] or nuclear energy [5] for several decades. In structural engineering, uncertainty quantification is mainly related to the design and optimization problems [7, 10, 24, 25, 12, 21], geotechnics [13] or system and parameter identification [23]. Furthermore, relevant benchmarks are known in nuclear energy [3], geosciences [2], control problems [17] or structural health monitoring [23]. These benchmark studies on special problems usually help comparing diverse methods and approaches with respect to their efficiency and accuracy and developing a standard.

Regarding the simultaneous consideration of aleatory and epistemic uncertainties, some investigations [6] and open challenge problems [18, 1] also exist. However, benchmarks dealing

with polymorphic uncertainties in structural engineering with focus on decision making and design are very rare. The recent test bed example [19] originates from a joint activity of the Priority Programme SPP 1886 of the German Research Foundation (DFG) entitled "Polymorphic uncertainty modeling for the numerical design of structures". The goal is an objective comparison of various descriptions of epistemic uncertainties with respect to decision making in engineering problems under polymorphic uncertainties.

The present contribution proposes a benchmark of a structural engineering problem that pursues several typical goals: (i) encourage researchers to develop new methods for polymorphic uncertainty modeling, (ii) provide a problem description and a measurement data set to test such new methods under realistic conditions, and (iii) allow an objective comparison of proposed methods based on a true data set of input and output. At that, the authors realize the need for a benchmark that would consider interpretable uncertainty for decision making based on the polymorphic uncertainty.

The considered engineering system is a portal frame under vertical and horizontal point loads, see Section 2. It is a simple mechanical system that helps avoiding false interpretation of results with respect to system behavior and failure states. Two competing failure modes, material failure and stability failure, make the limit state function strongly nonlinear and sensitive to uncertainties. Such a combination of failure modes is typical for many structural systems. Data for the structural and loading parameters are available more or less sparsely in Section 3. Using these information, three challenges formulated in Section 4 have to be solved. One of the crucial issues is an objective comparison of results caused by different underlying models for the uncertain input parameters. Obviously, this could be done on the basis of the decisions made. The second challenge of the benchmark deals with the question how data assimilation can help in the decision making. Finally, a design problem under polymorphic uncertainty is posed in which more demanding operation requirements have to be fulfilled. Reference solutions are given for comparison in Section 5 which have been determined by using the "true" structural and loading parameters which are only known to the authors. Final remarks can be found in Section 6.

## 2   Computational model

### 2.1   Reference structure: portal frame

A portal frame structure consisting of two columns of height $H$ and one girder of length $L$ (Fig. 1) is considered. Such frames are typical for many technical systems, for example industrial facilities or portal cranes. The columns are fixed in the foundation and the joints between columns and girder are rigid. The frame is loaded by a vertical crane force $F_V$ which can be located arbitrarily between two limit positions and is always directed in positive $z$-direction. The operational field of this force is marked gray in Fig. 1. In addition, the crane truck can cause a horizontal brake force $F_B$ at the same position as $F_V$. The direction of $F_B$ could be either in positive or negative $x$-direction. Finally, the left column is loaded horizontally by a force $F_H$ acting always in positive $x$-direction. The position of $F_H$ is fixed.

All loads are considered as static in order to exclude dynamic effects. That assumption is not far from reality since the crane operation is relatively slow and the frame structure is stiff enough, so that resonance effects and impulse loading can be neglected. The wind load is also considered as a static pressure for simplicity. Dynamic effects could be subject of the future study.

The columns and the girder are made of steel and have rectangular cross-sections of the same width and different heights, as shown in Fig. 1. Real hollow steel profiles are not considered here for simplicity, since the cross-sections cannot be varied continuously but taken from an assortment list at disposal. The material behavior is assumed to be linear elastic until failure.
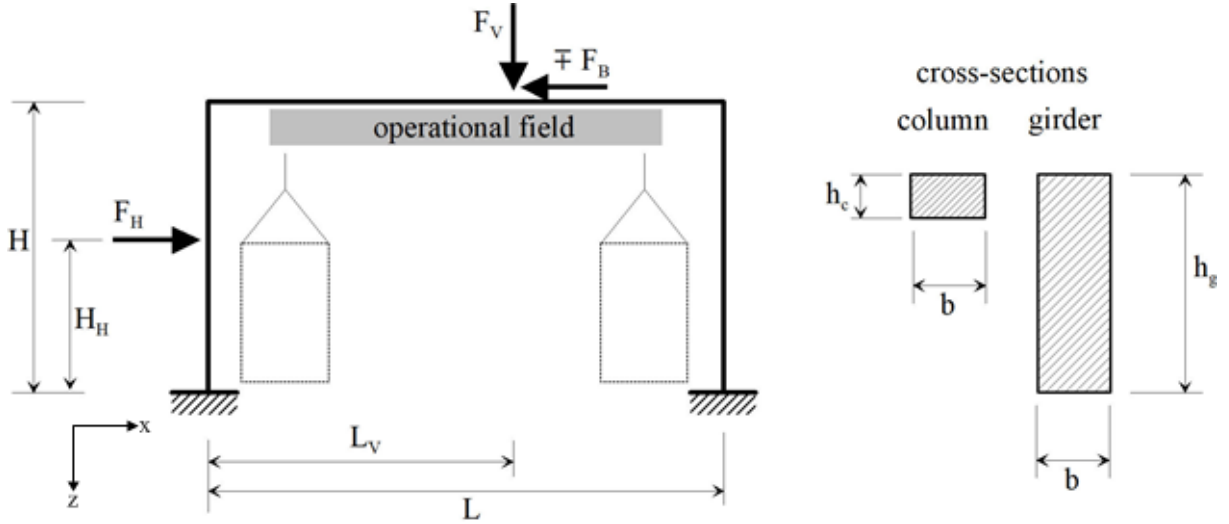
Figure 1: Mechanical model of the portal frame

## 2.2   Potential failure modes

It is assumed that the frame suffers only deformations in the plane, i.e. no out-of-plane deformations are considered. Under given loads, the frame experiences both normal forces $N$, lateral forces $Q$ and bending moments $M$. Typical distributions of these internal forces as well as a typical deformation state are given exemplarily in Fig. 2 for better understanding of system behavior. Two failure modes with respect to ultimate limit states are considered: material failure and stability failure.
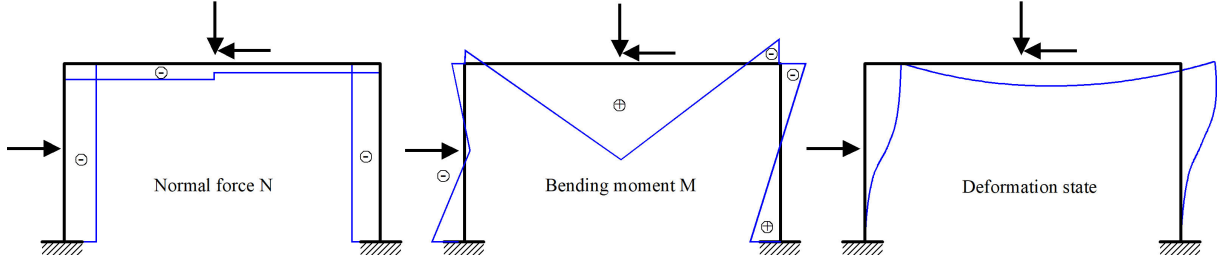


Figure 2: Internal forces $N$ and $M$ as well as deformation state of the portal frame

**Material failure (local stress problem)**   The material failure is always local and occurs due to the violation of a limit stress, in this case, the yield stress of steel $\sigma_\mathrm{y}$. The maximum acting stress can be calculated from the known normal forces and bending moments in each cross-section. According to Eurocode 3 [8], the simplified check of the yield stress can be performed by use of normal forces N and bending moments M as follows:

$$\sigma_\mathrm{max} = \frac{N}{A} \pm \frac{M}{W}, \tag{1}$$

with the cross-section area $A$ and the resistance moment $W$ of a rectangular cross-section according to Fig. 1

$$A = bh \quad \text{and} \quad W = \frac{bh^2}{6}. \tag{2}$$

The neglecting of the shear force is a conservative simplification that is acceptable for the present study due to a full rectangular cross-section of the columns and the girder. The influence of the shear force is expected to be quite small.

The limit state function for material failure is implicit since it requires each time the calculation of internal forces and corresponding maximum stresses at critical locations:

$$g\left(\sigma_{\max}, \sigma_{\mathrm{y}}\right) = \frac{\sigma_{\mathrm{y}}}{|\sigma_{\max}|} - 1.0 = \frac{\lambda_{\mathrm{mat}}}{\lambda} - 1.0 = 0. \tag{3}$$

Here, $\lambda_{\mathrm{mat}}$ and $\lambda$ indicate the critical load factor for material failure and the current load factor $\lambda = 1.0$, respectively.

**Stability failure (global buckling)**  The stability failure occurs due to the loss of the system equilibrium and is, therefore, always global. Stability failure is typically characterized by the buckling load $\lambda_{\mathrm{stab}}P$ and the buckling mode $\Phi$, i.e. the deformation state appearing after buckling. At that, the load factor $\lambda_{\mathrm{stab}}$ marks the critical value of a given load case $P$. A typical buckling mode of the portal frame under consideration is shown in Fig. 3.
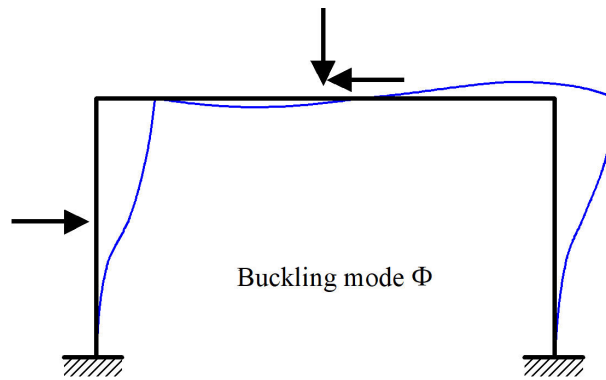


Figure 3: Buckling mode of the portal frame

The corresponding limit state function is also implicit since it requires a step of the system stability analysis and can be written in terms of the buckling load $\lambda_{\mathrm{stab}}P$ and a given load $\lambda P$ as follows:

$$g\left(\lambda, \lambda_{\mathrm{stab}}\right) = \frac{\lambda_{\mathrm{stab}}}{\lambda} - 1.0 = 0. \tag{4}$$

**System failure (material or stability failure)**  It is assumed that any local exceedance of yield stress and any buckling of the frame are unacceptable limit states for the crane operation and, thus, correspond to the system failure. The load, structural and material parameters in this benchmark are chosen in such a way that both material and stability failure occur at similar load levels. Therefore, the real failure mode is sensitive to uncertainties.

## 2.3  Structural analysis

Structural analysis of the frame is carried out by the displacement method [16] similarly to the finite element method. All necessary explanations are given below and provided in the appendix to the benchmark [20], so that all participants can use the same computational model. Thus, the model uncertainty can be excluded from this test aiming at the role of polymorphic data uncertainties.

The stiffness relation of the Bernoulli beam elements

$$
K_e \cdot v_e =
\begin{bmatrix}
\frac{EA}{l} & 0 & 0 & -\frac{EA}{l} & 0 & 0 \\
 & \frac{12EI}{l^3} & -\frac{6EI}{l^2} & 0 & -\frac{12EI}{l^3} & -\frac{6EI}{l^2} \\
 & & \frac{4EI}{l} & 0 & \frac{6EI}{l^2} & \frac{2EI}{l} \\
 & & & \frac{EA}{l} & 0 & 0 \\
 & & & & \frac{12EI}{l^3} & \frac{6EI}{l^2} \\
\text{symm.} & & & & & \frac{4EI}{l}
\end{bmatrix}
\cdot
\begin{bmatrix}
u_l \\ w_l \\ \varphi_l \\ u_r \\ w_r \\ \varphi_r
\end{bmatrix}
=
\begin{bmatrix}
N_l \\ Q_l \\ M_l \\ N_r \\ Q_r \\ M_r
\end{bmatrix}
= s_e
\tag{5}
$$

with the stiffness matrix $K_e$, the internal forces $s_e$ and the nodal displacement vector $v_e$ is well known [4]. It provides exact solution with respect to displacements:

$$
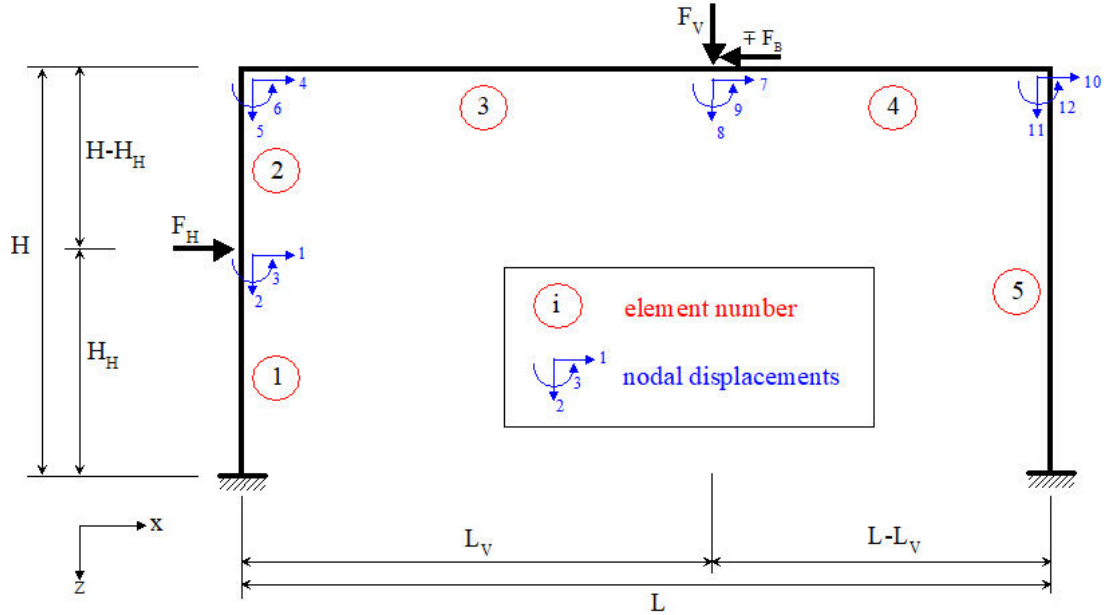v_e = K_e^{-1} \cdot s_e.
\tag{6}
$$



Figure 4: Discretized mechanical model with five beam elements and 12 nodal degrees-of-freedom

The portal frame is discretized by five classical Bernoulli beam elements and 12 active degrees-of-freedom (nodal displacements and rotations), as shown in Fig. 4. Its linear response to static loads can be calculated by use of the system stiffness relation, i.e. system of algebraic equations:

$$
K \cdot V = \lambda P \quad \text{with} \quad \lambda = 1.
\tag{7}
$$

The elastic system stiffness matrix $K_{ij}, i, j = 1, \ldots, 12$ and the system load vector $P_i, i = 1, \ldots, 12$ are derived analytically according to the system discretization in Fig. 4 and stay explicitly for all participants at disposal. A MATLAB® file executing an exemplary deterministic calculation is available in [20] in order to minimize mistakes and misunderstanding with respect to the structural analysis.

At that, the following input parameters are defined: material properties $E$, $\sigma_y$; geometry $L$, $H$; element cross-sections $b = b_1 = \ldots = b_5$, $h_c = h_1 = h_2 = h_5$, $h_g = h_3 = h_4$; load magnitudes $F_V$, $F_B$, $F_H$ and load positions $L_V$, $H_H$.

**Material failure (local stress problem)**   The analysis steps for evaluating the limit state function according to Eq. (3) are shortly described in the following:

1. calculate the system nodal displacements: $V = K^{-1} \cdot P$

2. transform the system displacements $V$ to the local element ones $v_{\mathrm{e},i}$

3. calculate the internal forces of each element: $s_{\mathrm{e},i}$ according to Eq. (5)

4. calculate the maximum stress in Eq. (1) of each element: $\sigma_{\max,i}$

5. calculate the maximum stress in portal frame: $\sigma_{\max} = \max(\sigma_{\max,i})$

6. calculate the critical load factor $\lambda_{\mathrm{mat}} = \frac{\sigma_y}{|\sigma_{\max}|}$

7. calculate the limit state function value according to Eq. (3): $g\left(\sigma_{\max}, \sigma_{\mathrm{y}}\right)$

**Stability failure (global buckling)**   If the frame losses its stability and buckles, it takes a new deformed state called buckling mode. The critical load at which it happens is called buckling load. The buckling load factor $\lambda$ and the buckling mode $\Phi$ can be calculated according to the classical stability theory from the generalized eigenvalue problem for the elastic $(K)$ and the geometric $(K_{\mathrm{g}})$ system stiffness matrices as follows:

$$(K - \lambda K_{\mathrm{g}})\Phi = 0. \tag{8}$$

The geometric system stiffness matrix $K_{\mathrm{g}}$ of the frame accounts for the deformed state and depends on the acting normal forces $N_i$ and, thus, on the load level $\lambda P$. The linearized geometric stiffness matrix $K_{\mathrm{g,e}}$ for classical beam elements is well known [4]. The geometric system stiffness matrix $K_{\mathrm{g}}$ of the frame with respect to 12 active nodal degrees-of-freedom (Fig. 4) is derived analytically by the authors from the element matrices $K_{\mathrm{g,e}}$ and stays at disposal for all participants. This kind of stability analysis provides only a linearized prediction of the buckling load and does not account for imperfections. However, it is considered as sufficient for the purpose of the present benchmark.

The analysis steps for evaluating the stability limit state function according to Eq. (4) are shortly described in the following:

1. calculate normal forces from the linear elastic analysis at $\lambda = 1.0$: $N_i$

2. calculate the geometric system stiffness matrix: $K_{\mathrm{g}}$

3. solve the eigenvalue problem in Eq. (8) and determine the minimum eigenvalue, i.e. load factor: $\lambda_{\mathrm{stab}} = \min(\lambda_i)$

4. calculate the limit state function $g\left(\lambda, \lambda_{\mathrm{stab}}\right)$ according to Eq. (4).

## 2.4   Result interpretation

Material failure occurs if $g(\sigma_{\max}, \sigma_{\mathrm{y}}) \leq 0$, stability failure takes place if $g\left(\lambda, \lambda_{\mathrm{stab}}\right) \leq 0$. The failure mode with the smallest load factor $\lambda_{\mathrm{stab}}$ or $\lambda_{\mathrm{mat}}$ occurs first.

# 3   Available data

The material, geometry, cross-section and loading parameters are generally considered with uncertainties. Some of them are assumed to be deterministic for simplicity. The model parameters are summarized in Table 1 and described below.

Table 1: Model parameters (d=deterministic, u=uncertain)

| Material | $E$: u | $\sigma_\mathrm{y}$: u | | | |
|---|---|---|---|---|---|
| Geometry | $L$: d | $H$: d | | | |
| Cross-sections | $b$: u | $h_\mathrm{c}$: u | $h_\mathrm{g}$: u | | |
| Loads | $F_\mathrm{V}$: u | $L_\mathrm{V}$: u | $F_\mathrm{B}$: u | $F_\mathrm{H}$: u | $H_\mathrm{H}$: d |

## 3.1   Material

It is known that the frame is built of steel S 355 [8] with the characteristic value of the yield strength of $275\,\mathrm{N/mm^2}$, that is the 5%-quantile value of the statistical distribution. The mean value of the Young's modulus $E$ can be taken as $210000\,\mathrm{N/mm^2}$. According to the Probabilistic Model Code [14], log-normal distributions are recommended to be applied with a coefficient of variation of 7% for the yield strength $\sigma_\mathrm{y}$ and with a coefficient of variation of 3% for the Young's modulus $E$.

## 3.2   Geometry and cross-sections

The lengths of the columns and the girder are explicitly measured and considered as deterministic: $L = 10\,\mathrm{m}$ and $H = 8\,\mathrm{m}$ (see Fig. 1). The quality management of the manufacturer gives a usual fabrication tolerance of $\pm 2\,\mathrm{mm}$ for the cross-sections of the frame. According to the original design, the cross-sections of the members should be as follows:

- width: $b = 0.20\,\mathrm{m}$

- heights: $h_\mathrm{c} = h_1 = h_2 = h_5 = 0.14\,\mathrm{m}$, $h_\mathrm{g} = h_3 = h_4 = 0.85\,\mathrm{m}$.

## 3.3   Loads

The operational field of the vertical load $F_\mathrm{V}$ is defined deterministically within two limit positions from the left edge $L_\mathrm{V} \in [2.0\,\mathrm{m},\, 8.0\,\mathrm{m}]$ (Fig. 1). The position $L_\mathrm{V}$ of the vertical load within this interval can be arbitrary. It is known that usual live loads of the crane vary between $1000\,\mathrm{kN}$ and $2000\,\mathrm{kN}$. A special sensor prevents the crane operation if the vertical load is larger than $3000\,\mathrm{kN}$.

The crane also causes brake loads when moving freight. Depending on the movement velocity and type of braking, the brake force can be determined with regard to the vertical force as follows:

$$|F_\mathrm{B}| = \alpha F_\mathrm{V} \quad \text{with} \quad \alpha \in [0.0001,\, 0.001] \,. \tag{9}$$

The brake force $F_\mathrm{B}$ can be directed both in positive and negative $x$-direction, while the vertical load $F_\mathrm{V}$ is directed always in positive $z$-direction.

The horizontal load $F_\mathrm{H}$ results from the wind and attacks the frame always at the fixed position $H_\mathrm{H} = 4.0\,\mathrm{m}$ in positive $x$-direction. During two separate measurement campaigns, each of five months duration, extreme values of the wind load $F_\mathrm{H}$ per month have been measured, see Table 2. The dead load of the portal frame is ignored for simplicity.

Table 2: Measured extreme loads $F_\mathrm{H}$

| Measurement 1 | 7.0 kN | 2.8 kN | 5.8 kN | 8.3 kN | 10.3 kN |
|---|---|---|---|---|---|
| Measurement 2 | 10.1 kN | 4.6 kN | 12.4 kN | 8.2 kN | 15.7 kN |

## 4   Challenges

The present benchmark proposes 3 challenges to deal with. Challenge 1 concerns the decision making about the permission for the crane operation under polymorphic uncertainties. Challenge 2 deals with the same decision but in the situation, if measurements on structural response without failure are available in addition. Application of data assimilation approaches is expected to correct the decision. Challenge 3 considers the structural optimization under polymorphic uncertainty in order to fulfill a low failure rate and to minimize material volume.

### 4.1   Challenge 1: Decision making

The engineering decision to be taken sounds: Is the operation of the frame under conditions described above allowed or not? The participants are expected to give the answer "yes" or "no". The answer "yes" is correct, if the failure rate remains smaller than $10^{-3}$, i.e. 1 failure per $10^3$ load operations, that is the requirement of the operator. The answer "no" is correct, if the failure rate is larger than $10^{-3}$. Besides the answer "yes" or "no", participants are expected to explain their classification of uncertainties, suitable approaches to handle them and the background of the decision.

In a second step, the decision can be improved by using $N = 5000$ data sets for the loading parameters $F_H$, $F_B$ and $F_V$. These are given in a text file in [20].

A reference probabilistic solution calculated by the authors with "true" distributions of the structural and loading parameters is given in Section 5.1 and can be used for an independent check of the decision by every participant.

### 4.2   Challenge 2: Decision making by data assimilation

The engineering decision to be taken sounds: Is the operation of the frame under conditions described above allowed, if the measurement data available from the operation is taken into account? The participants are expected to give the answer "yes" or "no". The answer "yes" is correct, if the failure rate remains smaller than $10^{-3}$, i.e. 1 failure per $10^3$ load operation. The answer "no" is correct, if the failure rate is larger than $10^{-3}$. The focus of this challenge is directed towards the data assimilation and its contribution to the uncertainty quantification. The "true" material and cross-sectional parameters are expected to be identified and specified. Again, a reference probabilistic solution is given for an independent check in Section 5.2.

**Operation measurement data**   During operation, that means without occurrence of failure, the response parameters given in Table 3 have been measured in addition to the associated loading parameters $F_H$, $F_B$ and $F_V$, see the text file in [20]. These data sets have been generated numerically, by calculating the frame with the "true" structural parameters. Several measurement errors and measurement noise are already incorporated into the data sets.

Table 3: Measurements during operation

| Measured value | Designation |
|---|---|
| horizontal displacement [m] | $V_4$ |
| vertical displacement [m] | $V_8$ |
| position of the vertical load [m] | $L_V$ |

**Remarks to the measurement data**   Due to the stiffness relations in the frame, it can be assumed that the whole girder experiences the same horizontal displacement. The vertical displacement $V_8$ is measured at the measured load position $L_V$, so both values belong together in each measurement. All measurements have been performed by a laser distance meter, which

provides a nominal accuracy of $\pm 1$mm. It is also known that some measurements could be disturbed by foreign objects breaking the laser rays during measurements. In this case, measurements contain wrong values.

## 4.3   Challenge 3: Design under uncertainties

The final challenge is to design the frame in such a way that the failure rate becomes smaller than $10^{-4}$. The only design parameters are the cross-section heights of the two columns $h_c$ and that of the girder $h_g$. All other parameters are the same as in challenge 1. The best design is that one with the minimum weight of the frame and the target failure rate fulfilled. In Section 5.3, the authors have calculated the optimal design values $h_{c,opt}$ and $h_{g,opt}$ by use of probabilistic methods with "true" distributions of the structural and loading parameters.

# 5   Reference solution

In the following, the authors of this benchmark offer reference solutions for each of the presented challenges. Participants are able to check their individual results and possibly improve their approaches. The reference solutions have been determined by stochastic simulations of the frame with "true" structural and loading parameters, which are known to the authors. This means that all uncertainties have been reduced as far as possible and epistemic uncertainties are not present anymore [15]. The uncertainties could be characterized as aleatory, so the reference solutions are based on classical probability theory.

## 5.1   Challenge 1: Decision making

According to the description of the input parameters in Section 3, the "true" probabilistic distributions have been prescribed by the authors and summarized in Table 4, see also Fig. 5.

Table 4: "True" distributions of the structural and loading parameters

| Input | Distribution |
|---|---|
| $E$ [N/m$^2$] | log-normal:   $E \sim \mathcal{LN}(\mu, \sigma) = \mathcal{LN}(210 \cdot 10^9, 6.3 \cdot 10^9)$ |
| $\sigma_y$ [N/m$^2$] | log-normal:   $\sigma_y \sim \mathcal{LN}(\mu, \sigma) = \mathcal{LN}(309.27 \cdot 10^6, 21.65 \cdot 10^6)$ |
| $b$ [m] | normal, truncated on $[l, u]$: |
|  | $b \sim \mathcal{TN}(\mu, \sigma, l, u) = \mathcal{TN}(0.200, 0.001, 0.198, 0.202)$ |
| $h_c$ [m] | normal, truncated on $[l, u]$: |
|  | $h_c \sim \mathcal{TN}(\mu, \sigma, l, u) = \mathcal{TN}(0.140, 0.001, 0.138, 0.142)$ |
| $h_g$ [m] | normal, truncated on $[l, u]$: |
|  | $h_g \sim \mathcal{TN}(\mu, \sigma, l, u) = \mathcal{TN}(0.850, 0.001, 0.848, 0.852)$ |
| $L_V$ [m] | uniform:   $L_V \sim \mathcal{U}(l, u) = \mathcal{U}(2, 8)$ |
| $F_V$ [N] | empirical:   see Fig. 5 |
|  | $\text{pdf}(0 \cdot 10^6 \leq F_V \leq 1 \cdot 10^6) = 0.5 \cdot 10^{-30} F_V^4$ |
|  | $\text{pdf}(1 \cdot 10^6 \leq F_V \leq 2 \cdot 10^6) = 0.6 \cdot 10^{-6}$ |
|  | $\text{pdf}(2 \cdot 10^6 \leq F_V \leq 3 \cdot 10^6) = -0.6 \cdot 10^{-12} F_V + 1.8 \cdot 10^{-6}$ |
| $\alpha$ [/] | uniform:   $\alpha \sim \mathcal{U}(l, u) = \mathcal{U}(0.0001, 0.001)$ |
| $F_B$ [N] | empirical:   $F_B = \pm \alpha F_V$ |
| $F_H$ [N] | Weibull:   $F_H \sim \mathcal{W}(a, b) = \mathcal{W}(10.6 \cdot 10^3, 2.5)$ |

Performing a plain Monte-Carlo simulation with $N = 10^6$ samples leads to the failure probability of:

$$p_F \approx 3.7 \cdot 10^{-3}\,. \tag{10}$$
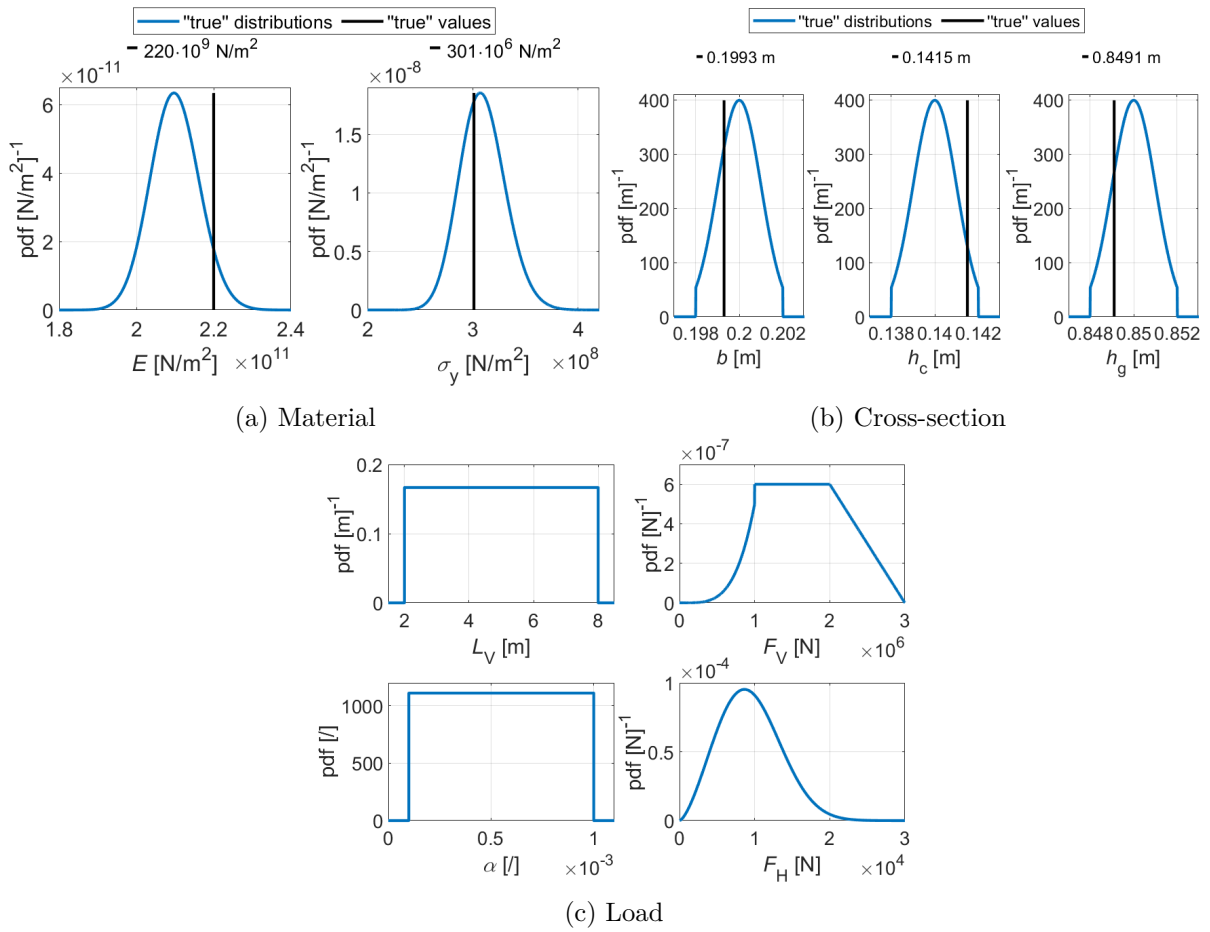
(a) Material

(b) Cross-section

(c) Load

Figure 5: Reference input parameters

Since $p_F$ is greater than the given threshold value of $1 \cdot 10^{-3}$, the operation of the frame is not allowed.

In case of system failure, that means $\min\{g(\sigma_{\max}, \sigma_y), g(\lambda, \lambda_{\text{stab}})\} \leq 0$, the material failure is to 49% and the stability failure to 51% the responsible failure mode.

## 5.2   Challenge 2: Decision making by data assimilation

**"True" structural parameters**   Within the bounds of the given "true" distributions of the structural parameters, the following "true" parameters have been defined by the authors, see also Fig. 5:

- Young's modulus: $E = 220 \cdot 10^9 \,\text{N/m}^2$

- yield strength: $\sigma_{\text{y}} = 301 \cdot 10^6 \,\text{N/m}^2$

- cross-section width: $b = 0.1993 \,\text{m}$

- cross-section height of the columns: $h_{\text{c}} = 0.1415 \,\text{m}$

- cross-section height of the girder: $h_{\text{g}} = 0.8491 \,\text{m}$

Again, a Monte-Carlo simulation with $N = 10^6$ samples has been performed, leading to the failure probability of:

$$p_F \approx 4.7 \cdot 10^{-4}\,. \tag{11}$$

If the "true" structural parameters could be perfectly identified by using available measurement data, than the operation of the frame could be allowed, that follows from the comparison of $p_F$ to the given limit value of $1 \cdot 10^{-3}$. If system failure has been occurred, then it has been initiated completely by material failure. The limit state function value for stability failure $g(\lambda, \lambda_{\mathrm{stab}})$ remains in this case always positive.

**Identification of the "true" structural parameters**  For the data assimilation process a text file with 5000 measurements of $V_4\,[\mathrm{m}]$, $V_8\,[\mathrm{m}]$, $L_V\,[\mathrm{m}]$, $F_H\,[\mathrm{N}]$, $F_B\,[\mathrm{N}]$ and $F_V\,[\mathrm{N}]$ is given [20]. The displacement measurement data of $V_4\,[\mathrm{m}]$, $V_8\,[\mathrm{m}]$ and the crane load location $L_V\,[\mathrm{m}]$ are noisy. The noise $r$ is normally distributed and truncated on $[l, u]$: $r \sim \mathcal{TN}(\mu, \sigma, l, u) = \mathcal{TN}(0\,\mathrm{m}, 0.001\,\mathrm{m}, -0.001\,\mathrm{m}, 0.001\,\mathrm{m})$. Additionally, 500 measurements in the data set have been further manipulated. All of those measurements could be gained from the sensors, thus, no system failure has occurred during measurements.

Before the data assimilation is initiated some preprocessing of the measurement data is necessary to delete corrupted ones. Most of them can be identified visually as shown in Fig. 6a. Note, that not all of the manipulated data in $L_V$ can be identified that will lead to small errors in the prediction of $V_8$.



(a) Identification of corrupted data

(b) Adaption of displacements

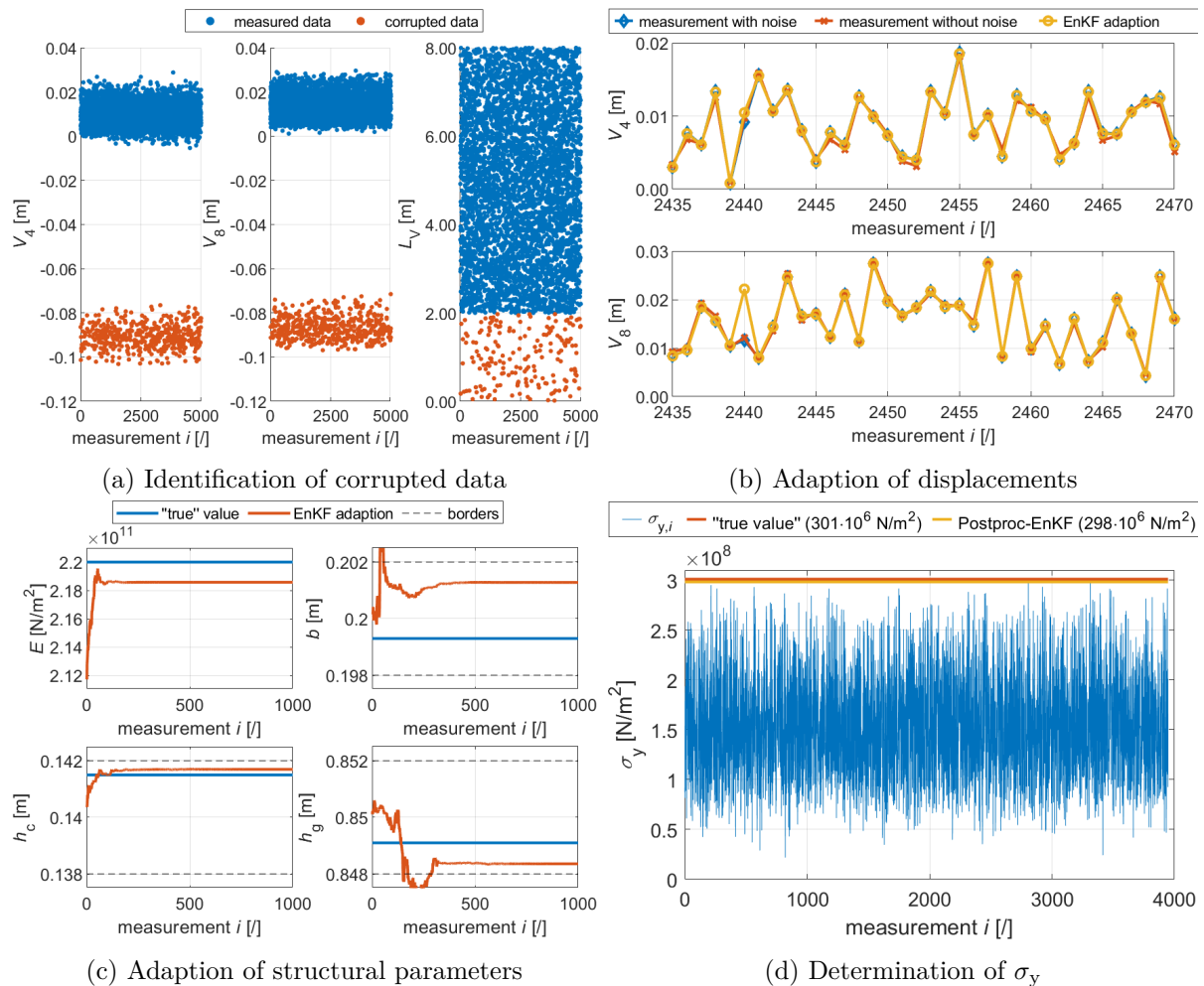(c) Adaption of structural parameters

(d) Determination of $\sigma_y$

Figure 6: Parameter identification by data assimilation

An augmented Ensemble Kalman Filter (EnKF) [11] has been used for the data assimilation process. This algorithm predicts the measured state variables $V_4$ and $V_8$ and the unknown structural parameters $E$, $b$, $h_c$ and $h_g$ at the same time for the measured loads and the crane load location $L_V$. The EnKF provides a very good prediction of the displacements $V_4$ and $V_8$,

see Fig. 6b. Due to an infinite number of combinations between $E$, $b$, $h_c$ and $h_g$ leading to the same entries in the stiffness matrix $K$, the prediction of the unknown structural parameters is acceptable but not optimal, see Fig. 6c. The results have been obtained with an ensemble size of 20 samples.

Some postprocessing of the adapted parameters is necessary to determine the value of $\sigma_y$. Since no system failure has been occurred during measurement, $\sigma_y$ has to be equal or larger than the maximum of each necessary $\sigma_{y,i}$ in measurement $i$ resulting in an acceptable prediction of the "true" $\sigma_y$, see Fig. 6d.

The identified structural parameters are summarized in Table 5. By use of these parameters, the resulting failure probability has been calculated to $p_F \approx 5.3 \cdot 10^{-4} < 1 \cdot 10^{-3}$. Therefore, the operation of the frame can be allowed.

Table 5: Comparison of "true" and identified structural parameters

| Parameter | "True" value | Identified value | Deviation |
|---|---|---|---|
| $E\,[\mathrm{N/m^2}]$ | $220.00 \cdot 10^9$ | $218.57 \cdot 10^9$ | $-0.7\%$ |
| $\sigma_y\,[\mathrm{N/m^2}]$ | $301.00 \cdot 10^6$ | $298.21 \cdot 10^6$ | $-0.9\%$ |
| $b\,[\mathrm{m}]$ | $0.1993$ | $0.2013$ | $+1.0\%$ |
| $h_c\,[\mathrm{m}]$ | $0.1415$ | $0.1417$ | $+0.1\%$ |
| $h_g\,[\mathrm{m}]$ | $0.8491$ | $0.8484$ | $-0.1\%$ |

## 5.3  Challenge 3: Design under uncertainties

The optimization problem is defined as

$$z_{\mathrm{opt}} = \min_{(h_c, h_g) \in \mathbb{R}^2_{>0}} \left\{ z\left(h_c, h_g\right) \mid p_F\left(h_c, h_g\right) < p_{\mathrm{T}} \right\} . \tag{12}$$

The objective function $z = 2h_c H + h_g L$ is proportional to the weight of the frame: $z \sim m = \rho V = \rho(2A_c H + A_g L) = \rho b z$. The probability of failure $p_F$, also depending on the design variables $h_c$ and $h_g$, has to be smaller than the given target value of $p_{\mathrm{T}} = 10^{-4}$. In each iteration, the computational model has been evaluated by $N = 10^7$ samples in a plain Monte-Carlo simulation with unknown loading parameters as described in Section 5.1 for Challenge 1.

By taking the material parameters $(E, \sigma_y)$ and the cross-section width $b$ as uncertain like in Section 5.1, the optimal values $h_{c,\mathrm{opt}} = 0.1449\,\mathrm{m}$ and $h_{g,\mathrm{opt}} = 0.8925\,\mathrm{m}$ have been determined. Both optimal values $h_{c,\mathrm{opt}}$ and $h_{g,\mathrm{opt}}$ are larger than the given "true" values. At that, the objective function reaches the value of $z_{\mathrm{opt}} = 11.2434\,\mathrm{m^2}$.

# 6  Final remarks

The proposed benchmark and a probabilistic reference solution for a typical structural engineering system should help to clarify the benefit of the polymorphic uncertainty modeling for decision making and design optimization. Evidently, a combination of diverse uncertainty models requires significant additional computational efforts compared to a purely probabilistic framework. It is usually expected that such efforts provide a basis for better decisions which is at the moment neither evident nor really justified.

Besides the methods for the uncertainty and system modeling themselves, one of the crucial issues remains an objective comparison of results provided by different uncertainty models. It is an open problem which we hope to discuss on the basis of the submitted solutions to the benchmark. Obviously, it can be done by use of decisions made.

The second challenge of the benchmark deals with the question how data assimilation can help in decision making. On this way, the epistemic uncertainties could be essentially reduced,

as far as possible. However, dealing with epistemic uncertainties in data assimilation is the next challenge. Finally, a design optimization problem under polymorphic uncertainty is more demanding process than that with probabilistic methods only. Again, a basis of the objective comparison of various optimal solutions with respect to safety and efficiency is a matter of discussion. It is worth mentioning that several aspects have been simplified in the present benchmark, like dynamic effects, lateral forces or realistic steel profiles. They do not limit the goals of the present benchmark study and are intended to be taken into account in the future benchmarks.

Researchers dealing with uncertainty quantification are invited to participate in this benchmark study and submit their solutions to the corresponding author via e-mail (yuriy.petryna@tu-berlin.de) or at least to refer to this benchmark in case of separate publications. Each submitted solution will be registered and independently checked as described above. A joint publication including comparison of all submitted results will be prepared and discussed with the participants. The information on the benchmark as well as all necessary data are available in [20].

# Acknowledgements

# References

[1] The NASA Langley UQ Challenge on Optimization Under Uncertainty. https://uqtools.larc.nasa.gov/nasa-uq-challenge-problem-2020/.

[2] D. Arnold, V. Demyanov, D. Tatum, M. Christie, T. Rojas, S. Geiger, and P. Corbett. Hierarchical benchmark case study for history matching, uncertainty quantification and reservoir characterisation. *Computers & Geosciences*, 50:4 – 15, 2013.

[3] A. Aures, F. Bostelmann, M. Hursin, and O. Leray. Benchmarking and application of the state-of-the-art uncertainty analysis methods xsusa and shark-x. *Annals of Nuclear Energy*, 101:262 – 269, 2017.

[4] Z. P. Bažant and L. Cedolin. *Stability of Structures.* WORLD SCIENTIFIC, 2010.

[5] F. Bostelmann and G. Strydom. Nuclear data uncertainty and sensitivity analysis of the vhtrc benchmark using scale. *Annals of Nuclear Energy*, 110:317 – 329, 2017.

[6] J. Chen and Z. Wan. A compatible probabilistic framework for quantification of simultaneous aleatory and epistemic uncertainty of basic parameters of structures by synthesizing the change of measure and change of random variables. *Structural Safety*, 78:76 – 87, 2019.

[7] A. Csébfalvi. Structural optimization under uncertainty in loading directions: Benchmark results. *Advances in Engineering Software*, 120:68 – 78, 2018.

[8] DIN Deutsches Institut für Normung e.V. *DIN EN 1993, Eurocode 3: Bemessung und Konstruktion von Stahlbauten.* Beuth Verlag GmbH, 12 2010.

[9] S. J. Fletcher. *Data Assimilation for the Geosciences - From Theory to Application.* Elsevier, 2017.

[10] T. Gernay, R. V. Coile, N. E. Khorasani, and D. Hopkin. Efficient uncertainty quantification method applied to structural fire engineering computations. *Engineering Structures*, 183:1 – 17, 2019.

[11] S. Gillijns, O. B. Mendoza, J. Chandrasekar, B. L. R. De Moor, D. S. Bernstein, and A. Ridley. What is the ensemble kalman filter and how well does it work? In *2006 American Control Conference*, pages 4448–4453, June 2006.

[12] M. Guedri, S. Cogan, and N. Bouhaddi. Robustness of structural reliability analyses to epistemic uncertainties. *Mechanical Systems and Signal Processing*, 28:458 – 469, 2012.

[13] M. Huber. Reducing forecast uncertainty by using observations in geotechnical engineering. *Probabilistic Engineering Mechanics*, 45:212 – 219, 2016.

[14] JCCS: Joint Committee on Structural Safety. *Probabilistic Model Code, Part 3, Resistance Models.* 3.02: Structural steel. Technical University of Denmark, 3 2001.

[15] A. D. Kiureghian and O. Ditlevsen. Aleatory or epistemic? does it matter? *Structural Safety*, 31(2):105 – 112, 2009.

[16] K. Knothe and H. Wessels. *Finite Elemente: Eine Einführung für Ingenieure.* Springer Berlin Heidelberg, 2017.

[17] I. Koryakovskiy, M. Kudruss, R. Babuška, W. Caarls, C. Kirches, K. Mombaur, J. P. Schlöder, and H. Vallery. Benchmarking model-free and model-based optimal control. *Robotics and Autonomous Systems*, 92:81 – 90, 2017.

[18] W. L. Oberkampf, J. C. Helton, C. A. Joslyn, S. F. Wojtkiewicz, and S. Ferson. Challenge problems: uncertainty in system response given uncertain parameters. *Reliability Engineering and System Safety*, 85(1):11 – 19, 2004.

[19] I. Papaioannou, M. Daub, M. Drieschner, F. Duddeck, M. Ehre, L. Eichner, M. Eigel, M. Götz, W. Graf, L. Grasedyck, R. Gruhlke, D. Hömberg, M. Kaliske, D. Moser, Y. Petryna, and D. Straub. Assessment and design of an engineering structure with polymorphic uncertainty quantification. *GAMM-Mitteilungen*, 42(2):e201900009, 2019.

[20] Y. Petryna and M. Drieschner. Data for: Decision making in structural engineering problems under polymorphic uncertainty - a benchmark proposal. Mendeley Data, v4, 2019. http://dx.doi.org/10.17632/jw3wj5kwh2.4.

[21] G. Schuëller and H. Pradlwarter. Benchmark study on reliability estimation in higher dimensions of structural systems – an overview. *Structural Safety*, 29(3):167 – 182, 2007.

[22] J. Slingo and T. Palmer. Uncertainty in weather and climate prediction. *Philosophical Transactions of the Royal Society A: Mathematical, Physical and Engineering Sciences*, 369:4751 – 4767, 2011.

[23] K. Worden, R. Barthorpe, E. Cross, N. Dervilis, G. Holmes, G. Manson, and T. Rogers. On evolutionary system identification with applications to nonlinear benchmarks. *Mechanical Systems and Signal Processing*, 112:194 – 232, 2018.

[24] H. Zhai and J. Zhang. Equilibrium reliability measure for structural design under twofold uncertainty. *Information Sciences*, 477:466 – 489, 2019.

[25] Y. Zhang, Y. Lu, Y. Zhou, and Q. Zhang. Resistance uncertainty and structural reliability of hypar tensioned membrane structures with pvc coated polyesters. *Thin-Walled Structures*, 124:392 – 401, 2018.